The expression of TGFβ signal transducers in the hypodermis regulates body size in *C. elegans*

Jianjun Wang, Rafal Tokarz and Cathy Savage-Dunn*

Department of Biology, Queens College, and The Graduate School and University Center, CUNY, Flushing, NY 11367, USA
*Author for correspondence (e-mail: cathy_savage@qc.edu)

SUMMARY

In *C. elegans*, a TGFβ-related signaling pathway regulates body size. Loss of function of the signaling ligand (*dbl-1*), receptors (*daf-4* and *sma-6*) or Smads (*sma-2*, *sma-3* and *sma-4*) results in viable, but smaller animals because of a reduction in postembryonic growth. We have investigated the tissue specificity of this pathway in body size regulation. We show that different tissues are reduced in size by different proportions, with hypodermal blast cell size most closely proportional to body size. We show that SMA-3 Smad is expressed in pharynx, intestine and hypodermis, as has been previously reported for the type I receptor SMA-6. Furthermore, we find that SMA-3::GFP is nuclear localized in all of these tissues, and that nuclear localization is enhanced by SMA-6 activity. Interestingly, SMA-3 protein accumulation was found to be negatively regulated by the level of Sma/Mab pathway activity. Using genetic mosaic analysis and directed expression of SMA-3, we find that SMA-3 activity in the hypodermis is necessary and sufficient for normal body size. As *dbl-1* is expressed primarily in the nervous system, these results suggest a model in which postembryonic growth of hypodermal cells is regulated by TGFβ-related signaling from the nervous system to the hypodermis.

Key words: Body size, TGFβ, BMP, Smad, *Caenorhabditis elegans*

INTRODUCTION

The TGFβ superfamily, which includes TGFβ, BMPs and activins, regulates cell growth and differentiation in both vertebrates and invertebrates (reviewed by Massagué, 1998; Raftery and Sutherland, 1999; Hill, 2001; Savage-Dunn, 2001). Signaling initiates when the ligand binds to the type II and type I receptors, both of which are Ser/Thr kinases. During this process, the type II receptor phosphorylates the type I receptor. The activated type I receptor phosphorylates the cytoplasmic Smads. Upon phosphorylation, Smads form a heteromeric complex, translocate into the nucleus and regulate the transcription of downstream genes (Heldin et al., 1997; Wrana and Attisano, 2000; Massagué and Wotton, 2000; Patterson and Padgett, 2000). The Smads are thus the critical intracellular signal transducers for TGFβ-related signaling.

Smads are separated into three categories, R-Smad, Co-Smad and anti-Smad. R-Smad activity is regulated by the receptors by phosphorylation. Co-Smads are not activated by phosphorylation, but cooperate with R-Smads to form a functional complex. The anti-Smads negatively regulate the TGFβ pathway, and their expression is dependent upon TGFβ signaling (Massagué and Chen, 2000). The structure of a Smad comprises conserved MH1 and MH2 domains, separated by a variable linker region. The MH1 domain has the DNA-binding region and nuclear localization sequence (Shi et al., 1998; Xiao et al., 2000). The MH2 domain contains an SSXS motif that is phosphorylated by type I receptor on the last two serines (Souchelnytskyi et al.,

1997). Once phosphorylated, the activated R-Smad forms a heterodimer or heterotrimer with the Co-Smad (Shi et al., 1997; Wu et al., 2001; Qin et al., 1999; Qin et al., 2001).

In the nematode *Caenorhabditis elegans*, there are two characterized TGFβ-related pathways, the Dauer pathway and the Sma/Mab (small/male tail abnormal) pathway (Patterson and Padgett, 2000; Savage-Dunn, 2001). The Dauer pathway controls entry into and exit from the dauer stage, an L3 larval stage specialized for harsh environmental conditions. Entry into the dauer stage is regulated by environmental cues, such as the availability of food, the population density and temperature. The Dauer pathway is composed of the ligand (*daf-7*), the type II receptor (*daf-4*), the type I receptor (*daf-1*) and the Smads (*daf-8*, *daf-14* and *daf-3*). Loss of function of any factor except *daf-3* results in the dauer constitutive phenotype, in which worms enter dauer even under favorable conditions (Estevez et al., 1993; Ren et al., 1998; Gunther et al., 2000; Inoue and Thomas, 2000). However, the absence of *daf-3* activity gives a dauer defective phenotype, in which worms do not form dauers (Patterson et al., 1997).

The ligand for the Sma/Mab pathway, *dbl-1*, is related to *Drosophila dpp* and vertebrate BMPs (Suzuki et al., 1999; Morita et al., 1999). It functions with the type II receptor *daf-4* and the type I receptor *sma-6* (Estevez et al., 1993; Krishna et al., 1999). The Dauer and Sma/Mab pathways use a common type II receptor, *daf-4*. In the Sma/Mab pathway, *daf-4* and *sma-6* receptors activate the R-Smads, *sma-2* and *sma-3*. These are thought to form complexes with the Co-Smad, *sma-4*, to

propagate the signal into the nucleus (Savage et al., 1996; Savage-Dunn et al., 2000). Loss-of-function mutations in any of the Sma/Mab pathway components result in small body size. In addition, defects of the male tails are seen, including sensory ray fusions and crumpled spicules. Both of the R-Smad proteins, SMA-2 and SMA-3, are crucial for pathway function, suggesting the formation of a heteromeric complex containing two different R-Smad subunits (Savage-Dunn et al., 2000).

The underlying cause of the small body size phenotype is still poorly understood. In theory, the final size of an organ or organism can be determined by the regulation of cell number, cell size, or both. Cell number may be controlled by the regulation of cell division or of cell death. Cell size is usually coordinated with the cell cycle, and often correlates with ploidy (Galitski et al., 1999). Mutants of the Sma/Mab pathway provide an opportunity to study the molecular regulation of body size in a viable animal model. Previous reports (Suzuki et al., 1999; Flemming et al., 2000) and our own unpublished results (R. T. and C. S.-D., unpublished) indicate that these small mutants contain normal numbers of cells. Therefore, some or all cell sizes must be reduced. We have addressed the cell and tissue specificity of the Sma/Mab pathway regulation of body size in several ways. First, we measured individual cell and organ sizes in small mutants to determine which were reduced in size. Second, we characterized the expression and subcellular localization of SMA-3. We have previously reported that *sma-3* is widely expressed, based on a transcriptional *lacZ* fusion (Savage-Dunn et al., 2000). Here, we provide a higher resolution expression pattern using SMA-3::GFP translational fusions. We find that *sma-3* is expressed in the pharynx, intestine and hypodermis. Third, we used mosaic analysis and directed expression of *sma-3* to determine where it functions to regulate body size. These experiments indicate that the hypodermis is the crucial tissue involved in body size regulation.

MATERIALS AND METHODS

Worm strains

Wild type was *C. elegans* strain N2, from which all of the mutants were isolated. Unless otherwise noted, strains were grown at 20°C. All strains used in experiments were cultured as described previously (Brenner, 1974). The following mutations were used: LGII, *sma-6(wk7)*; LGIII, *sma-2(e502), sma-3(wk30), sma-4(e729)*; LGV, *dbl-1(wk70)*, *sma-1(e30)* and *him-5(e1490)*.

Small mutants chosen were either known null mutants or the most severe mutants available. *sma-6(wk7)* has an early stop codon in the extracellular region that results in a null mutation (Krishna et al., 1999). There is an early termination in the DBL-1 bioactive domain in *dbl-1(wk70)* mutants (Suzuki et al., 1999). An arginine in the beginning of the linker region in SMA-3 mutates into a stop codon, suggesting *sma-3(wk30)* is a strong allele (Savage-Dunn et al., 2000). In *sma-2(e502)*, the mutation G372D disrupts a critical amino acid in the *sma-2* MH2 domain (Savage et al., 1996). The DNA sequence of the canonical *sma-4(e729)* allele had not previously been determined. We therefore sequenced the *sma-4* gene from these mutants. Fragments of the *sma-4* gene were amplified by PCR and directly sequenced. *sma-4(e729)* contains a single nucleotide substitution resulting in a Q246 (CAA) to stop (UAA) mutation. Therefore, *sma-4(e729)* is an early termination mutation.

Construction of *sma-3* and GFP fusion genes

An 8 kb *sma-3* genomic fragment was obtained from the cosmid R13F6 by digesting with *Pst*I and subcloning into the vector pBLUESCRIPT SK+ (pCS29). This construct rescues *sma-3(wk30)* mutants. To create GFP fusion constructs, *Mlu*I restriction sites were created in the *sma-3*-coding region, after the start codon (pCS185) or before the stop codon (pCS186) independently, by site-directed mutagenesis (MutaGene kit from BioRad). A GFP *Mlu*I fragment from pPD118.90 (A. Fire) was subcloned into the newly generated *Mlu*I sites, forming two *sma-3::gfp* translational fusion constructs; N-terminal GFP (pCS170) or C-terminal GFP (pCS171). We also created a *sma-3* construct lacking all coding sequences. An *Xho*I-*Mlu*I fragment from pCS185 containing *sma-3* upstream sequences was ligated into *Xho*I-*Mlu*I-digested pCS186 in which upstream and coding regions had been removed leaving only downstream sequences. This *sma-3* construct (pCS210) therefore contains upstream and downstream noncoding sequences but no coding region.

Fusion of tissue specific promoters and *sma-3::gfp* coding region

The promoters used in tissue specific expression of *sma-3::gfp* included *elt-3, vha-7, dpy-7* (hypodermal); *elt-2, vha-6* (intestine); *myo-2* (pharynx); and the third isoform of *tmy-1*(pharynx and intestine) (Gilleard et al., 1999; Oka et al., 2001; Gilleard et al., 1997; Okkema et al., 1993; Fukushige et al., 1998; Anyanful et al., 2001). The *elt-2* and *elt-3* promoters were kindly provided by R.W. Padgett's laboratory (HW373 and HW375). The others were obtained by PCR using N2 genomic DNA as template from worm lysates. The PCR primers used were:

> *tmy-1*f, 5′-AAGTCGACCGAGTAGGTCTCGCCACG-3′;
> *tmy-1*r, 5′-ATTCTGCAGAAGTCAGAGGTGT-3′;
> *myo-2*f, 5′-AAGTCGACCTCTCCGATTGCTATCATG-3′;
> *myo-2*r, 5′-AACTGCAGTGTCTGACGATCGAGGGTT-3′;
> *dpy-7*f, 5′-AAGTCGACTGGCGCAAGAGGCAGTGC-3′;
> *dpy-7*r, 5′-AACTGCAGTTATCTGGAACAAAATGTAAGA-3′;
> *vha-7*f, 5′-AAGTCGACAGGAAATTGTGAGAAG-3′;
> *vha-7*r, 5′-AACTGCAGATTACGTCGTTGGTGGA-3′;
> *vha-6*f, 5′-AATCTAGAGCATGTACCTTTATAGG-3′; and
> *vha-6*r, 5′-AACCCGGGTAGGTTTTAGTCGCCCTG-3′.

After the PCR products were digested by the appropriate restriction enzymes, the promoters were cloned into pBLUESCRIPT SK+ vector. Next, a *Pst*I fragment containing the *sma-3::gfp(N)*-coding region was excised from pCS170 (one *Pst*I site derives from the GFP vector pPD118.90) and inserted into vectors containing the heterologous promoters. Thus, after translation, each of the protein products has GFP at the N terminus and SMA-3 at the C terminus.

Transformation and integration

Transformation of constructs into worms was carried out by microinjection (Mello et al., 1991). Unless otherwise stated, the injection solution contains 20 ng/μl of experimental plasmid and 100 ng/μl pRF4 (*rol-6* plasmid). The co-injection of *vha-6::sma-3* and *myo-2::sma-3* includes 20 ng/μl of each. The co-injection of C-terminal *sma-3::gfp* (pCS171) with pCS29, pCS170 or pCS210 contains 10 ng/μl of each experimental plasmid.

We used γ-rays to integrate the *sma-3::gfp(N)* array into *sma-3(wk30)* and the co-injected *sma-3::gfp(C)* with *sma-3* genomic and *sma-3::gfp(C)* with *sma-3* non-coding arrays into N2. More than 100 L4 or young adult worms with each extra-chromosomal array were picked. After exposure to a cesium source, the worms were separated into 20 plates (five worms in each). After starvation, the worms were chunked into new plates. We allowed the worms to recover for 2 days. Each worm carrying the array was picked into a separate plate. After one generation, plates with 100% worms containing the reporter gene (*rol-6*) were selected. The integrated arrays are *qcIs6[sma-3::gfp(N) + rol-6]*, *qcIs12[sma-3::gfp(C)+ sma-3 + rol-6]* and *qcIs16[sma-3::gfp(C)+ sma-3no-code + rol-6]*.

Table 1. Cell and organ size measurements in *sma* mutant animals at the L3 stage

Strain	Seam cell length (μm)	Seam cell area (μm²)	*n* (cells)	Pharynx length (μm)	Body length (μm)	*n* (worms)
N2	31.8±3.7	1.18±0.13	104	106.1±4.2	615±20	16
dbl-1	25.0±3.8	1.02±0.14	106	101.4±5.0	515±30	16
sma-3	25.5±3.3	1.01±0.09	103	99.1±4.3	512±23	16
sma-4	24.7±3.2	0.99±0.12	115	99.9±4.4	518±22	16
sma-1	28.0±4.1	1.08±0.17	74	71.2±6.9	462±35	13

Data are given as mean±standard deviation. All three measurements were performed on a single set of animals for each genotype.

Length measurements

To characterize the small phenotype, we measured seam cells, pharynx length and body length in the same animals. The *jam-1::gfp* marker (Mohler et al., 1998) was used to visualize seam cells. This marker localizes to the adherens junctions surrounding these lateral hypodermal cells. *jam-1::gfp* was also introduced into *sma-1*, *sma-3*, *sma-4* and *dbl-1* mutants by standard genetic crosses. L3 larvae were picked and the seam cells were observed under fluorescence. The seam cell lineage is highly dynamic and involves major changes in cell shape. We focused on worms containing rectangularly shaped cells, after they completed their divisions. We looked for worms with at least four consecutive cells ideal for measurement. Once ideal worms were found, the seam cells were photographed using a 40× objective. The pharynx and the entire worm were photographed using a 10× objective. The measurements were performed using SigmaScan software.

To assess body length in transgenic animals, cultures were synchronized by bleaching gravid hermaphrodites in order to isolate eggs. These eggs were introduced onto new plates. The body length was measured after 96 hours, in the adult stage. Transgenic (rolling) worms were picked, mounted on slides and measured as described above.

Mosaic analysis

Mosaic analysis was performed with strains containing high copies of a plasmid pTG96 (generously provided by Min Han). The plasmid contains a fusion of the ubiquitously expressed, nuclear localized sur-5 with GFP (Yochem et al., 1998). The *sur-5::gfp* was co-injected with the *sma-3* rescuing clone pCS29 into *sma-3*(wk30) animals. Two lines were obtained, with strain designations CS122 *sma-3(wk30);qcEx26* and CS125 *sma-3(wk30);qcEx27*. The extragenic arrays have rescuing activity. The strains were then observed under fluorescence for mosaicism at a magnification of 400×. Both small and wild-type mosaic animals were analyzed.

Western blot

Worms were washed off non-starved plates and frozen at –80°C overnight. The boiling buffer (8% SDS+20 mM DTT+100 mM pH 6.8 Tris+10 mM PMSF) was added and the samples were boiled for 5 minutes. The protein concentration was determined and equal amounts of total protein were loaded in each lane. After running the SDS-PAGE gel, the proteins were transferred onto nitrocellulose membrane. The membrane was blocked by 5% BSA in PBS and probed by rabbit anti-GFP antibody (Clontech). The secondary antibody (anti-rabbit) and detection solutions were from the ECL western blotting analysis system (Amersham).

RESULTS

Cell and organ size measurements in TGFβ Sma/Mab mutants

TGFβ Sma/Mab mutants are the same size as wild-type animals at hatching, but grow more slowly during larval stages and are about half the length of wild type in adulthood (Savage-Dunn et al., 2000), as well as being thinner (data not shown). This reduction in body size could in principle be due either to reduced cell number or to reduced cell size, or both. Others have reported no significant change in the number of nuclei in *dbl-1(wk70)*, *daf-4(m63)* and *sma-2(e502)* mutants compared with N2 (Suzuki et al., 1999; Flemming et al., 2000). We also find no difference in the number of nuclei in a *dbl-1(wk70)* mutant (data not shown). These results indicate that the small body size phenotype must be due to a reduction in size of some or all of the cells in the animal.

We have measured two accessible tissues to determine the extent of cell size reduction in small animals. The seam cells are lateral hypodermal blast cells that donate daughter nuclei to the hypodermal syncytium after each cell division, and eventually fuse in adults (Sulston and Horvitz, 1977). We took advantage of the *jam-1::gfp* marker (Mohler et al., 1998), which localizes to the adherens junctions surrounding the seam cells. The seam cell marker was crossed into *sma* mutant backgrounds and fluorescence was observed in the L3 stage. By this stage, *sma* mutant worm length is significantly different from wild type (Savage-Dunn et al., 2000); at later stages the seam cells will fuse with each other and cannot be measured individually. The seam cells in mutant animals are shorter in length than the seam cells of wild-type animals (Table 1). In Sma/Mab mutants, the difference in seam cell length is proportional to the difference in overall body length (Fig. 1). It was possible that this reduction in seam cell length was offset by an increase in width, so we also measured seam cell area. Again, we found that seam cell area was reduced in Sma/Mab mutants (Table 1). For a negative control, we used *sma-1* mutants. *sma-1* mutants are also small, but they follow a different growth pattern than the TGFβ Sma/Mab mutants (Savage-Dunn et al., 2000). At the L3 stage, *sma-1* body length is less than the Sma/Mab pathway mutants, but the mean length and area of the seam cells is larger (Table 1).

We also measured the length of the pharynx in the same worms. Interestingly, in the TGFβ mutants the pharynx is smaller than in N2, but only slightly so, with the ratios varying between 0.93 and 0.96 of wild type (Table 1, Fig. 1). In *sma-1*, the pharynx is 33% smaller than wild-type. Thus, in the small mutants examined, different tissues are reduced in size by different proportions. In the TGFβ Sma/Mab mutants, but not in *sma-1* animals, the seam cell size is proportional to the body size.

Levels of functional activity of *sma-3::gfp* translational fusions

To determine the expression pattern and subcellular
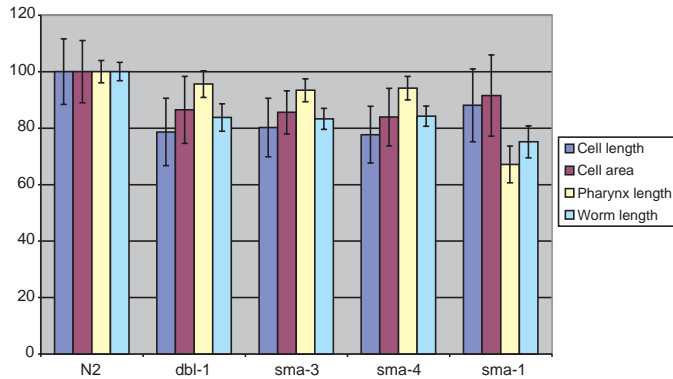
Fig. 1. Seam cell, pharynx and body length measurements of *dbl-1*, *sma-3*, *sma-4* and *sma-1* mutants as a proportion of wild-type (N2) size.

localization of SMA-3 Smad protein, we made two kinds of *sma-3::gfp* translational fusion gene constructs. In pCS170, GFP is inserted at the N terminus, and in pCS171, GFP is inserted at the C terminus. After transformation into *sma-3(wk30)*, the rescuing ability was assessed. Rescue of body size was assessed by measuring worm length 96 hours after embryo collection. Rescue of male tail patterning was assessed by determining the frequency of sensory ray fusions. In the wild-type *C. elegans* male tail are nine bilateral pairs of sensory organs, the sensory rays (Sulston et al., 1980). Each ray is characterized by its unique position, morphology and neurotransmitter usage. The Sma/Mab pathway plays a role in the specification of rays 5, 7 and 9. In mutants, these rays often display characteristics of rays 4, 6 and 8, respectively, resulting in readily observable fusions between rays 4-5, 6-7 and 8-9 (Savage et al., 1996; Suzuki et al., 1999; Morita et al., 1999; Krishna et al., 1999).

The N-terminal *sma-3::gfp* construct is functional, restoring most of the body length (Table 2) and rescuing the male tail sensory ray pattern (Table 3). However, the C-terminal construct has very little rescuing activity in body length (Table 2) and it only partially rescues male tail ray fusions (Table 3). When the extra-chromosomal array with the C-terminal

construct is crossed into a wild-type background, it even shows a slight inhibition in body length, but does not affect male tail development (Tables 2 and 3), suggesting that it can interfere with wild-type SMA-3 function. The R-Smad C-terminal SSXS motif is the site of phosphorylation and may participate in intermolecular interactions (Wu et al., 2001; Qin et al., 2001). The C-terminal insertion of GFP may disrupt some of these interactions.

sma-3::gfp fusion gene expression pattern and protein localization

Both the N-terminal functional and the C-terminal nonfunctional *sma-3::gfp* constructs show the same pattern of expression, but the level of fluorescence of the C-terminal construct is much higher. In Fig. 2, we show the expression of the *sma-3::gfp* C-terminal construct. Expression begins late in embryogenesis, and continues through larval stages into adulthood. In larvae, expression is strong in the hypodermis, pharynx and intestine. *sma-3* expression in the hypodermis is seen throughout the large hypodermal syncytium hyp7, but not in the lateral hypodermal blast cells (the seam cells). Nuclear accumulation in all of these tissues is strong. This nuclear localization does not depend on the activity of *sma-6*, however (see Fig. 6E,F).

Expression of the N-terminal construct is similar, although much weaker, even after integration (Fig. 3A). Again, the nuclear fluorescence is prominent in the pharynx, intestine and hypodermis. We asked whether the nuclear accumulation depends on the activity of other components in the pathway. When the integrated N-terminal construct array (*qcIs6*) was crossed into *sma-4(e729)* (Fig. 3C) or *sma-2(e502)* (Fig. 3E) mutant backgrounds, the nuclear localization did not change significantly. This result is consist with previous reports that R-Smad nuclear translocation does not require complex formation with a co-Smad partner (Liu et al., 1997). When the array is crossed into *sma-6(wk7)* mutants, the protein became evenly distributed between the cytoplasm and the nucleus in many but not all animals (Fig. 3G). Thus, the nuclear accumulation of SMA-3::GFP is enhanced by but not dependent on activation by the type I receptor. Determining whether this extensive nuclear localization is characteristic of

Table 2. The function of tissue-specific *sma-3* expression constructs in body length regulation

Genotype	Transgene	GFP expression*	Length (mm)[†]	*n* (worms)
Wild type N2	*qcEx50[rol-6]*	NA	1.15±0.11	44
sma-3(wk30)	*qcEx50[rol-6]*	NA	0.74±0.05	40
sma-3(wk30)	*qcEx24[sma-3::gfp(N)+rol-6]*	H+P+I	1.05±0.08	38
sma-3(wk30)	*qcEx42[sma-3::gfp(C)+rol-6]*	H+P+I	0.83±0.07	34
Wild type N2	*qcEx42[sma-3::gfp(C)+rol-6]*	H+P+I	1.03±0.10	51
sma-3(wk30)	*qcEx57[sma-3::gfp(C)+sma-3::gfp(N)+rol-6]*	H+P+I	1.00±0.11	40
sma-3(wk30)	*qcEx44[Pelt-3::sma-3+rol-6]*	hyp7	1.04±0.07	40
sma-3(wk30)	*qcEx55[Pvha-7::sma-3+rol-6]*	hyp7	1.02±0.06	42
sma-3(wk30)	*qcEx51[Pdpy-7::sma-3+rol-6]*	hyp7	0.94±0.10	32
sma-3(wk30)	*qcEx45[Pelt-2::sma-3+rol-6]*	Intestine	0.66±0.05	30
sma-3(wk30)	*qcEx53[Pvha-6::sma-3+rol-6]*	Intestine	0.67±0.04	32
sma-3(wk30)	*qcEx52[Pmyo-2::sma-3+rol-6]*	Pharynx	0.80±0.06	24
sma-3(wk30)	*qcEx54[Ptmy-1(III)::sma-3+rol-6]*	Pharynx+ Intestine	0.83±0.06	38
sma-3(wk30)	*qcEx56[Pmyo-2::sma-3+Pvha-6::sma-3+rol-6]*	Pharynx+ Intestine	0.80±0.05	27

*NA, not applicable, H+P+I means hypodermis, pharynx and intestine.
[†]The worms are measured 96 hours after synchronization by bleaching. The data shows the average length±standard deviation.
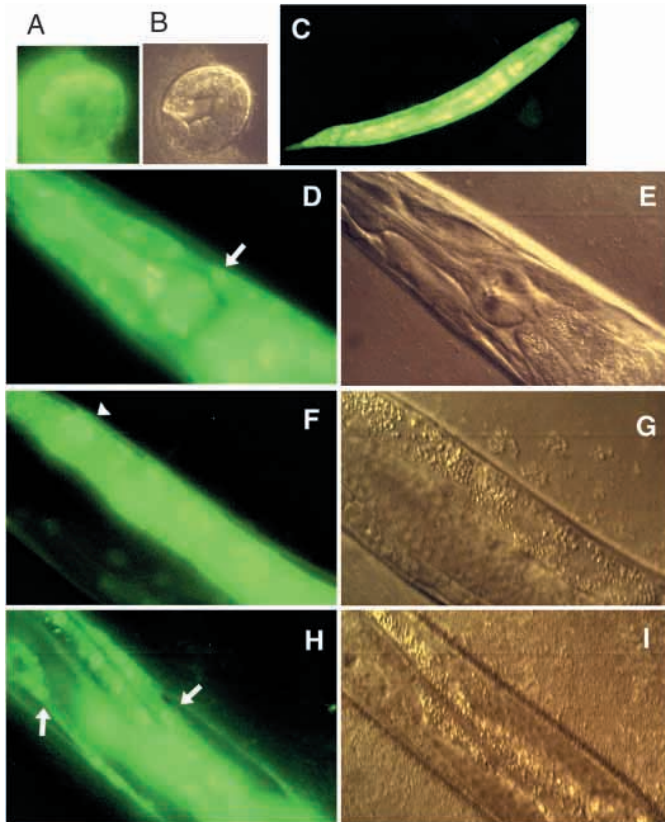
Fig. 2. The *sma-3::gfp(C)* expression stage and pattern in wild type. (A,C,D,F,H) Direct fluorescence from GFP; (B,E,G,I) Nomarski images of the same samples to their left. (A,B) The expression begins at the late embryo stage, 2.5-fold stage. (C) The gene expression pattern in L3 stage worms. At L4 stage, *sma-3* is expressed in pharynx, head region hypodermis (D,E), intestine (F,G) and body hypodermis (H,I). The arrows indicate the hypodermal nuclei. The arrowhead indicates an intestinal nucleus.
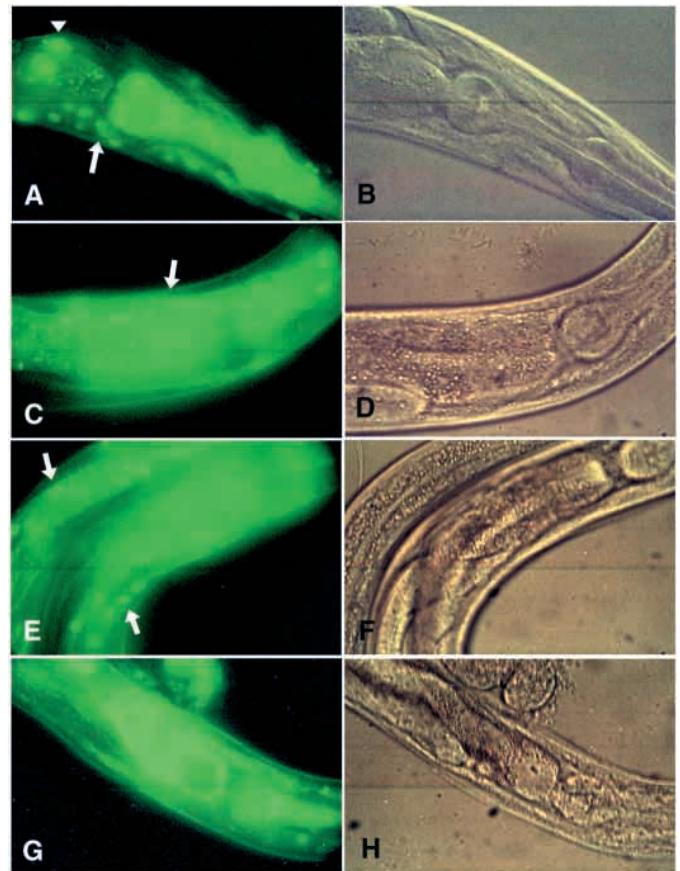
Fig. 3. The *sma-3:gfp(N)* expression and localization in different mutant backgrounds: (A,B) *sma-3(wk30)*; (C,D) *sma-4(e729)*; (E,F) *sma-2(e502)*; and (H,I) *sma-6(wk7)*. (A,C,E,H) show direct fluorescence from GFP; (B,D,F,I) are the Nomarski images of the same samples. The arrows indicate hypodermal nuclei (A,C,E). The arrowhead indicates an intestinal nucleus (A).

the endogenous SMA-3 protein must await the development of SMA-3 antibodies.

Mosaic analysis of *sma-3*

As SMA-3 expresses in the pharynx, intestine and hypodermis, we wished to determine the tissue in which its activity is crucial for regulation of body size. We first addressed this by mosaic analysis. The *sma-3* rescuing genomic fragment was injected with a ubiquitously expressed nuclear localized SUR-5::GFP marker (Yochem et al., 1998) into *sma-3(wk30)* mutants.

Animals inheriting the array are wild-type in length, while those without the array are small. Animals were screened for rare loss of the extrachromosomal array in somatic tissues (Table 4). Each tissue was scored as positive if any cells of the tissue expressed the construct.

We find that animals with loss of the array in the pharynx or the intestine have wild-type body size (Table 4). Rare small worms have also been isolated with expression in the intestine and/or the pharynx. Therefore, expression of SMA-3 in the intestine and the pharynx is neither necessary nor sufficient for

Table 3. The function of *sma-3::gfp* constructs in male tail patterning

| | Frequency of ray fusion (%) | | | |
Genotype and transgene	Rays 4 and 5	Rays 6 and 7	Rays 8 and 9	*n* (sides)
*him-5(e1490)**	0	0	6	35
*sma-3(wk30);him-5**	22	69	11	55
sma-3(wk30);him-5;qcEx24[sma-3::gfp(N)+rol-6]	0	0	5	148
sma-3(wk30);him-5;qcEx42[sma-3::gfp(C)+rol-6]	2	27	26	84
him-5;qcEx42[sma-3::gfp(C)+rol-6]	0	0	6	106
sma-3(wk30);him-5;qcEx57[sma-3::gfp(C)+sma-3::gfp(N)+rol-6]	0	6	5	64

*Savage-Dunn et al., 2000.

Table 4. Mosaic analysis of *sma-3*

	n (worms)	Intestine	Pharynx	Nerve cord	Nerve ring	Body muscle	Hypodermis
Wild type	4	–	+	+	+	+	+
	1	–	–	+	+	–	+
	2	–	–	–	–	+	+
	1	–	–	+	–	+	+
Small	1	+	+	–	–	–	–
	1	–	+	–	–	–	–
	1	+	–	–	–	+	–
	1	+	–	–	–	–	–

+, GFP expression in some cells of the tissue; –, no GFP expression in any cells of the tissue.

regulation of body size. However, expression of *sma-3* in the hypodermis appears to be vital for restoration of wild-type body size. We have not observed a mosaic worm of wild-type length without *sma-3* expression in the hypodermis. Conversely, we have not seen a small worm with hypodermal expression.

Effects of tissue-specific expression of *sma-3* on body length

To confirm the conclusions of the mosaic analysis and apply a quantitative measure of body length, we created transgenic animals with *sma-3* expression driven by heterologous promoters. Constructs were made with tissue-specific promoters and the *sma-3::gfp* N-terminal fusion. Four types of expression patterns were used. For hypodermal expression, we used *elt-3::sma-3* (Gilleard et al., 1999), *vha-7::sma-3* (Oka et al., 2001) and *dpy-7::sma-3* (Gilleard et al., 1997). These hypodermal promoters function in hyp7 but not in the seam cells. For pharyngeal expression, we chose *myo-2::sma-3* (Okkema et al., 1993). For intestinal expression, we used *elt-2::sma-3* (Fukushige et al., 1998) and *vha-6::sma-3* (Oka et

al., 2001). Finally, for simultaneous expression in the pharynx and intestine, we used *tmy-1* isoform III (Anyanful et al., 2001) as well as a combined injection of *myo-2::sma-3* and *vha-6::sma-3*. We confirmed the expression of SMA-3::GFP in the specified tissues by direct fluorescence (Fig. 4).

The hypodermal expression of *sma-3* from any of the three hypodermal promoters restores body length to the same extent as the *sma-3* native promoter (Table 2). When *sma-3* is only expressed in intestine, there is no effect on the body length. The pharyngeal expression or the co-expression in pharynx and intestine do not increase the body length significantly. Therefore, *sma-3* expression in the hypodermis is sufficient for the regulation of body length.

SMA-3 protein accumulation

We have found that the nonfunctional *sma-3::gfp* C-terminal construct gives a stronger fluorescent signal than the functional N-terminal construct (Fig. 5A-D). This difference in intensity was consistent in at least three independent lines for each construct (data not shown). We also tried lower (10 μg/ml) or higher (40 μg/ml) concentrations of the construct in injection mixtures, but the intensity of fluorescence was not different from that with 20 μg/ml (data not shown). The reduced fluorescence of the *sma-3::gfp(N)* construct could be due to changes in protein folding that affect GFP fluorescence or to reduced protein accumulation.

We hypothesized that the difference in fluorescence is due to differing levels of accumulation of the *sma-3::gfp(N)* and *sma-3::gfp(C)* fusion proteins. There are two possible causes of such differences in accumulation. First, the C-terminal construct could be inherently more stable. Second, SMA-3 degradation could be induced by *sma-3* activity in a negative-feedback loop. To solve this puzzle, we simply mixed the two *sma-3::gfp* constructs together (10 μg/ml each) and microinjected into *sma-3(wk30)* mutants. This mixture can
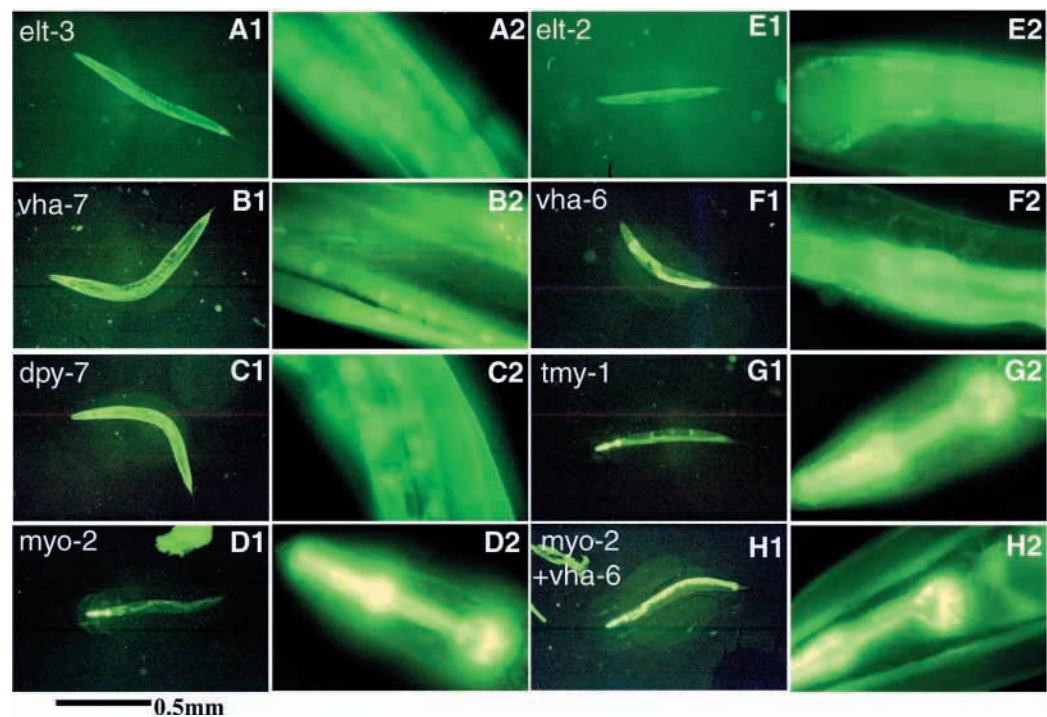
Fig. 4. The *sma-3* expression with tissue-specific promoters. Worms carrying each array are picked during L4 stage and photographed 24 hours later. The A1-H1 photos (first and third columns) show the overview of the expression pattern and the body size. The A2-H2 photos (second and fourth columns) focus on the region that has strong GFP expression. The tissue specific promoter used in each set is indicated in the A1-H1 photos. Scale bar: 0.5 mm in A1-H1 photos.
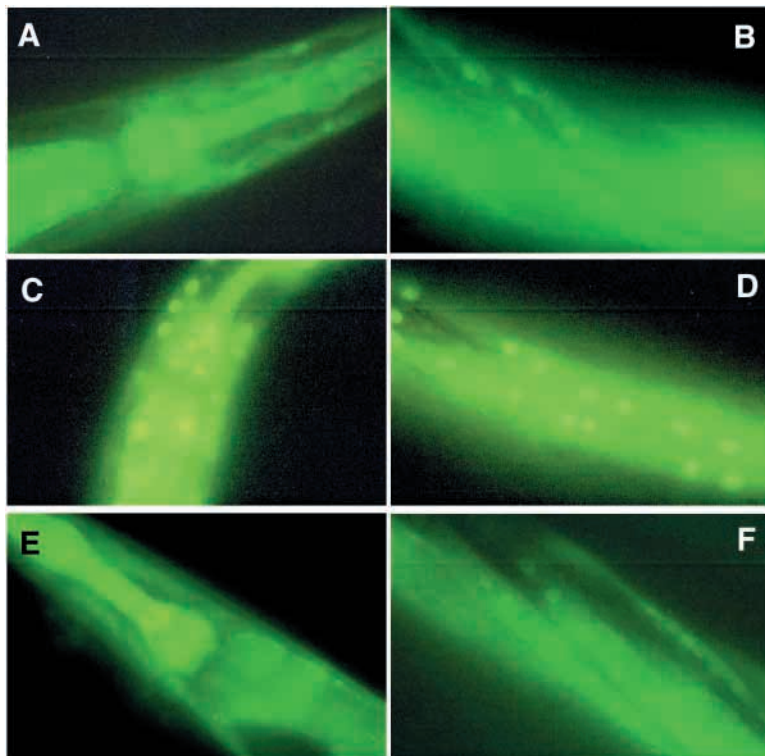
Fig. 5. The distinct intensity of fluorescence in worms with different *sma-3::gfp* constructs in the *sma-3(wk30)* background. (A,B) *sma-3::gfp(N);* (C,D) *sma-3::gfp(C);* (E,F) co-injection of *sma-3::gfp(N)* and *sma-3::gfp(C)*. (A,C,E) The head region; (B,D,F) the body hypodermis. All of the worms (L4 stage) are grown under the same conditions and the photos are taken with the same exposure time.

3::GFP(C) protein accumulation requires active Co-Smad and type I receptor, respectively. Consistent with the results from fluorescence in whole worms, SMA-3::GFP from *qcIs12* in the N2 background is almost undetectable (lane 1). By contrast, a strong band is detectable in the *qcIs16* strain (lane 4). In the *sma-4* (lane 2) and *sma-6* (lane 3) backgrounds, SMA-3::GFP levels from *qcIs12* increase relative to the levels in a wild-type background. These results are consistent with a negative-feedback loop regulating SMA-3 protein accumulation.
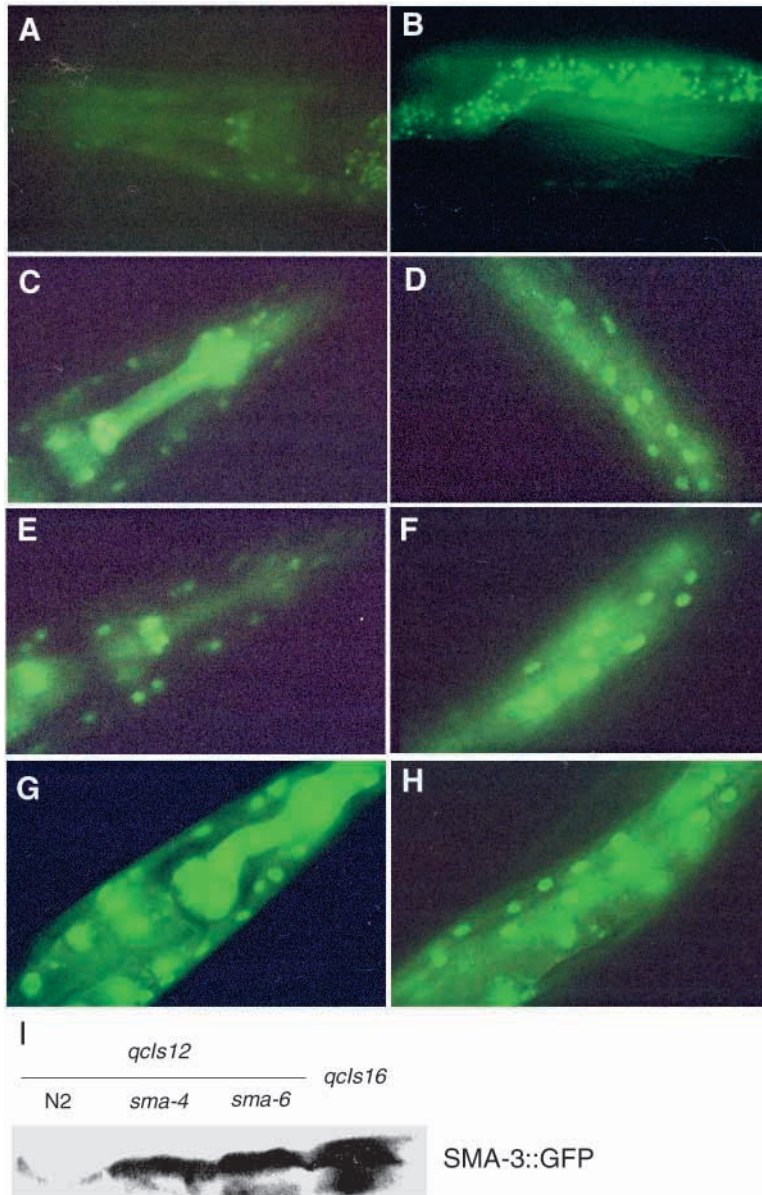
DISCUSSION

The Sma/Mab pathway acts in the hypodermis to regulate body length

The specification of body size is a poorly understood phenomenon. In recent years, studies have begun to address the molecular mechanisms governing size in animals such as *Drosophila* (Oldham et al., 2000; Johnston and Gallant, 2002; Martin-Castellanos and Edgar, 2002) and *C. elegans* (Flemming et al., 2000; Savage-Dunn et al., 2000). In *C. elegans*, most of the mutants resulting in small body size are defective in components of a TGFβ-related signaling pathway, the Sma/Mab pathway (Savage-Dunn, 2001). A limited number of additional loci that mutate to a small phenotype have been described (*sma-1*, *sma-5* and *sma-8*), the best studied of which is *sma-1*, a βH-spectrin homolog (McKeown et al., 1998). An effect of BMP family signaling on cell size may be conserved, as *Drosophila dpp* also regulates cell growth (Martin-Castellanos and Edgar, 2002).

We have previously shown that the Sma/Mab pathway functions postembryonically (Savage-Dunn et al., 2000), in contrast to the embryonic requirement for *sma-1* (McKeown et al., 1998). In this study, we have addressed the tissue specificity of the Sma/Mab pathway in body size regulation and find that the hypodermis is the crucial TGFβ-responsive tissue involved in body size regulation. The hypodermis of *C. elegans* forms the outer layer of cells surrounding the animal, and it secretes the cuticle (Johnstone, 2000). The largest region of the hypodermis is made up of a single multinucleate syncytium, hyp7 (Sulston and Horvitz, 1977). Two lateral rows of hypodermal blast cells, the seam cells, divide during each larval stage to form one daughter cell that fuses with hyp7 and one that remains in the seam. After fusion with hyp7, these nuclei undergo endoreduplication (Hedgecock and White, 1985; Flemming et al., 2000). Additional smaller hypodermal cells are present in the head (hyp1-hyp6) and the tail (hyp8-hyp12).

We conclude that Sma/Mab signal transduction functions in the hypodermis to regulate body size based on (1) the SMA-3

rescue the *sma-3* mutant, in both body length and male tail patterning (Tables 2 and 3). In other words, the mixture provides *sma-3* activity. However, the level of fluorescence is low, although the C-terminal construct is present (Fig. 5E,F). This implies that after adding the functional *sma-3* construct, the C-terminal fusion protein could be degraded by an unknown factor. This result also contradicts the model that the difference in fluorescence is due to differences in protein folding that affect GFP fluorescence.

We further tested this model by co-injecting the nonfunctional *sma-3::gfp(C)* (10 μg/ml) construct either with the functional *sma-3* genomic fragment (pCS29) (10 μg/ml) or with a *sma-3* construct in which the coding region had been deleted (pCS210) (10 μg/ml) that would not have SMA-3 activity. In the co-injection with *sma-3* genomic sequences, only a trace amount of GFP fluorescence can be seen (Fig. 6A,B). However, in the co-injection with pCS210, the level of fluorescence remains high (Fig. 6G,H). Thus, under a variety of conditions, *sma-3::gfp* fluorescence levels negatively correlate with SMA-3 activity levels. Finally, we addressed the question of whether a negative-feedback loop requiring other components of the pathway regulates SMA-3 protein accumulation. In fact, an extrachromosomal array carrying *sma-3::gfp(C)* and the *sma-3* genomic fragment shows increased levels of fluorescence in a *sma-4* or *sma-6* mutant background, suggesting that the feedback is dependent on an intact signaling pathway (Fig. 6C-F).

We verified these results in a western blot using anti-GFP antibody. The extrachromosomal arrays were integrated: *qcIs12* contains *sma-3::gfp(C)* and *sma-3* genomic, *qcIs16* contains *sma-3::gfp(C)* and *sma-3* non-coding genomic. *qcIs12* was crossed into the *sma-4(e729)* and *sma-6(wk7)* mutant backgrounds to determine whether loss of SMA-

Fig. 6. Expression of SMA-3::GFP C-terminal fusion protein in different genetic backgrounds. (A-F) *sma-3::gfp* C-terminal fusion was co-injected with *sma-3* genomic fragment, which contains the whole *sma-3* gene sequence. (A,B) *sma-3(wk30)* mutant background. (C,D) *sma-4(e729)* mutant background. (E,F) *sma-6(wk7)* mutant background. (G,H) *sma-3::gfp* C-terminal fusion was co-injected with *sma-3* genomic lacking coding sequences. All of the photos are taken with the same exposure time. The prominent fluorescence in B is autofluorescence of the intestine. (I) Western blot of total protein extracts from strains carrying *sma-3::gfp(C)* constructs. The extra-chromosomal arrays were integrated into N2 (*qcIs12[sma-3::gfp(C) + sma-3 + rol-6]* and *qcIs16[sma-3::gfp(C) + sma-3no-code + rol-6]*) and crossed into different genetic backgrounds. Equal amounts of total protein were loaded in each lane and SMA-3::GFP fusion protein was detected by western blot with anti-GFP antibody.

expression pattern; (2) cell and organ size measurements; (3) *sma-3* mosaic analysis; and (4) directed expression of *sma-3*. We have examined SMA-3 Smad expression and subcellular localization using SMA-3::GFP fusion constructs. SMA-3 is expressed in the pharynx, intestine and hypodermis. This expression pattern coincides with the expression pattern of the type I receptor SMA-6 (Krishna et al., 1999; Yoshida et al., 2001). In cell size measurements, we find that the seam cells in Sma/Mab mutants, but not the pharynx, show a reduction in size similar to the reduction in the body length. The relative maintenance of pharynx length in Sma/Mab mutants suggests that the expression of Sma/Mab signaling components in the pharynx may serve an unidentified role. We used mosaic analysis and tissue-specific expression of *sma-3* to determine in which tissues it is required for body size. Our results indicate that SMA-3 function in the hypodermis is necessary and sufficient for body size regulation. The hypodermal requirement for SMA-3 is consistent with the results from

similar experiments on the receptors *sma-6* (Yoshida et al., 2001) and *daf-4* (Inoue et al., 2000).

Although the seam cells are reduced in size in Sma/Mab mutants, the effect on the seam cells may not be cell autonomous, as neither *sma-3* (this study) nor *sma-6* (Yoshida et al., 2001) expression is detected in these cells. Furthermore, we have shown that *sma-3* expression from hyp7-specific promoters, which also do not express in the seam cells, is sufficient to rescue the body size in a *sma-3* mutant (Table 2). Because the seam cells and hyp7 are joined by gap junctions (D. Hall, personal communication) and adherens junctions (Mohler et al., 1998), there could be communication between these tissues without postulating additional extracellular signals. We speculate that in addition to the seam cells, the large hypodermal syncytium hyp7 may be reduced in volume in the small mutants. This hypothesis could be tested by electron microscopy. As *dbl-1* is expressed primarily in the nervous system (Suzuki et al., 1999), these results suggest a model in which postembryonic growth of hypodermal cells is regulated by TGFβ-related signaling from the nervous system to the hypodermis.

One important question that remains to be addressed is why these cells are smaller. Several possibilities may be considered. One is that reduced DNA content leads to smaller size. The nuclei of the *C. elegans* intestine and hypodermis normally undergo endoreduplication during larval growth (Hedgecock and White, 1985). In late adulthood the hypodermal nuclei in wild type have an average ploidy of 10.7C, and some nuclei have gone through two rounds of endoreduplication (Flemming et al., 2000). Furthermore, Flemming et al., found reduced ploidy in hypodermal cells of *daf-4* and *sma-2* mutants, 5.8 and 7.0 respectively. They proposed that this may be the reason for the smaller body size of Sma/Mab mutants, as ploidy can control cell size (Galitski et al., 1999). It is not yet clear, however, whether changes in ploidy are sufficient to explain the changes in body size.

Another mechanism that could contribute to smaller cell size is reduced protein synthesis. To test this hypothesis, we tried growing worms on the protein synthesis inhibitor cycloheximide to see if we could phenocopy the small defect.

At concentrations in which the worms could grow, however, they were normal in size. A third possibility is a change in the cell cycle. By speeding up the cell cycle, small cells could be generated such as is seen in yeast *wee* mutants (Futcher, 1996). Because the small mutants do not develop more quickly, however, any cell cycle defect could only be in some stage(s) of the cell cycle. Finally, metabolic changes could decrease cell size. In *Drosophila* (but not in *C. elegans*) mutations in insulin signaling result in small cells and small animals (Oldham et al., 2000). Similarly, some change in sugar or fat metabolism could underlie the small phenotype.

SMA-3 protein accumulation may be regulated by a feedback loop

Using different SMA-3::GFP fusion constructs, we have obtained evidence that SMA-3 protein accumulation is negatively regulated by the level of SMA-3 and Sma/Mab pathway activity. Furthermore, a negative-feedback loop is consistent with the lack of effect of overexpressing *sma-3*. The overexpression of *dbl-1* ligand induces a long phenotype and male tail sensory ray defects (Suzuki et al., 1999), while the overexpression of *sma-3* does not (data not shown). In other systems, it has been shown that Smads are degraded by the activity of Smurf E3 ubiquitin ligases (Zhu et al., 1999; Zhang et al., 2001; Podos et al., 2001). In human or *Xenopus*, Smurf-1 and Smurf-2 induce R-Smad degradation by the ubiquitin pathway (Zhu et al., 1999; Zhang et al., 2001). Through interaction with the anti-Smad Smad7, Smurf-1 can also induce the degradation of type I receptor (Ebisawa et al., 2001). Smurf-2 enhances the degradation of type I receptor (Kavsak et al., 2000) or SnoN oncogene (Bonni et al., 2001). The target is selected by the Smad with which it interacts. A Smurf gene, *Dsmurf* (*lack* – FlyBase) is found in *Drosophila*, where it negatively regulates *dpp* signaling in embryonic dorsoventral patterning (Podos et al., 2001). In *C. elegans*, we find several open reading frames with homology to human or *Xenopus* Smurf genes, allowing the possibility that one or more of these genes functions in the Sma/Mab pathway. It will be interesting to determine whether a Smurf gene participates in a negative feedback loop.

REFERENCES

Anyanful, A., Sakube, Y., Takuwa, K. and Kagawa, H. (2001). The third and fourth tropomyosin isoforms of Caenorhabditis elegans are expressed in the pharynx and intestines and are essential for development and morphology. *J. Mol. Biol.* **313**, 525-537.

Bonni, S., Wang, H. R., Causing, C. G., Kavsak, P, Stroschein, S. L., Luo, K. and Wrana, J. L. (2001). TGF-β induces assembly of a Smad2-Smurf2 ubiquitin ligase complex that targets SnoN for degradation. *Nat. Cell Biol.* **3**, 587-595.

Brenner, S. (1974). The genetics of *Caenorhabditis elegans*. *Genetics* **77**, 71-94.

Ebisawa, T., Fukuchi, M., Murakami, G., Chiba, T., Tanaka, K., Imamura, T. and Miyazono, K. (2001). Smurf1 interacts with transforming growth factor-β type I receptor through Smad7 and induces receptor degradation. *J. Biol. Chem.* **276**, 12477-12480.

Estevez, M., Attisano, L., Wrana, J. L., Albert, P. S., Massagué, J. and Riddle, D. L. (1993). The daf-4 gene encodes a bone morphogenetic protein receptor controlling *C. elegans* dauer larva development. *Nature* **365**, 644-649.

Flemming, A. J., Shen, Z. Z., Cunha, A., Emmons, S. W. and Leroi., A. M. (2000). Somatic polyploidization and cellular proliferation drive body size evolution in nematodes. *Proc. Natl. Acad. Sci. USA* **97**, 5285-5290.

Fukushige, T., Hawkins, M. G. and McGhee, J. D. (1998). The GATA-factor *elt-2* is essential for formation of the *Caenorhabditis elegans* intestine. *Dev. Biol.* **198**, 286-302.

Futcher, B. (1996). Cyclins and the wiring of the yeast cell cycle. *Yeast* **12**, 1635-1646.

Galitski, T., Saldanha, A. J., Styles, C. A., Lander, E. S. and Fink, G. R. (1999). Ploidy regulation of gene expression. *Science* **285**, 251-254.

Gilleard, J. S., Barry, J. D. and Johnstone, I. L. (1997). cis regulatory requirements for hypodermal cell-specific expression of the *Caenorhabditis elegans* cuticle collagen gene dpy-7. *Mol. Cell. Biol.* **17**, 2301-2311.

Gilleard, J. S., Shafi, Y., Barry, J. D. and McGhee, J. D. (1999). ELT-3: A *Caenorhabditis elegans* GATA factor expressed in the embryonic epidermis during morphogenesis. *Dev. Biol.* **208**, 265-280.

Gunther, C. V., Georgi, L. L. and Riddle, D. L. (2000). A *Caenorhabditis elegans* type I TGF β receptor can function in the absence of type II kinase to promote larval development. *Development* **127**, 3337-3347.

Hedgecock, E. M. and White, J. G. (1985). Polyploid tissues in the nematode *Caenorhabditis elegans*. *Dev. Biol.* **107**, 128-133.

Heldin, C. H., Miyazono, K. and ten Dijke, P. (1997). TGF-β signalling from cell membrane to nucleus through SMAD proteins. *Nature* **390**, 465-471.

Hill, C. S. (2001). TGF-β signalling pathways in early *Xenopus* development. *Curr. Opin. Genet. Dev.* **11**, 533-540.

Inoue, T. and Thomas, J. H. (2000). Targets of TGF-β signaling in *Caenorhabditis elegans* dauer formation. *Dev. Biol.* **217**, 192-204.

Johnston, L. A. and Gallant, P. (2002). Control of growth and organ size in *Drosophila*. *BioEssays* **24**, 54-64.

Johnstone, I. L. (2000). Cuticle collagen genes. Expression in *Caenorhabditis elegans*. *Trends Genet.* **16**, 21-27.

Kavsak, P., Rasmussen, R. K., Causing, C. G., Bonni, S., Zhu, H., Thomsen, G. H. and Wrana, J. L. (2000). Smad7 binds to Smurf2 to form an E3 ubiquitin ligase that targets the TGFβ receptor for degradation. *Mol. Cell.* **6**, 1365-1375.

Krishna, S., Maduzia, L. L. and Padgett, R. W. (1999). Specificity of TGFβ signaling is conferred by distinct type I receptors and their associated SMAD proteins in *Caenorhabditis elegans*. *Development* **126**, 251-260.

Liu, F., Pouponnot, C. and Massagué, J. (1997). Dual role of the Smad4/DPC4 tumor suppressor in TGFbeta-inducible transcriptional complexes. *Genes Dev.* **11**, 3157-3167.

Martin-Castellanos, C. and Edgar, B. A. (2002). A characterization of the effects of Dpp signaling on cell growth and proliferation in the Drosophila wing. *Development* **129**, 1003-1013.

Massagué, J. (1998). TGF-β signal transduction. *Annu. Rev. Biochem.* **67**, 753-791.

Massagué, J. and Chen, Y. G. (2000). Controlling TGF-β signaling. *Genes Dev.* **14**, 627-644.

Massagué, J. and Wotton, D. (2000). Transcriptional control by the TGF-β/Smad signaling system. *EMBO J.* **19**, 1745-1754.

McKeown, C., Praitis, V. and Austin, J. (1998). *sma-1* encodes a βH-spectrin homolog required for *Caenorhabditis elegans* morphogenesis. *Development* **125**, 2087-2098.

Mello, C. C., Kramer, J. M., Stinchcomb, D. and Ambros, V. (1991). Efficient gene transfer in *C. elegans*: extrachromosomal maintenance and integration of transforming sequences. *EMBO J.* **10**, 3959-3970.

Mohler, W. A., Simske, J. S., Williams-Masson, E. M., Hardin, J. D. and White, J. G. (1998). Dynamics and ultrastructure of developmental cell fusions in the *Caenorhabditis elegans* hypodermis. *Curr. Biol.* **8**, 1087-1090.

Morita, K., Chow, K. L. and Ueno, N. (1999). Regulation of body length and male tail ray pattern formation of Caenorhabditis elegans by a member of TGF-beta family. *Development* **126**, 1337-1347.

Oka, T., Toyomura, T., Honjo, K., Wada, Y. and Futai, M. (2001). Four subunit a isoforms of *Caenorhabditis elegans* vacuolar H+-ATPase. Cell-specific expression during development. *J. Biol. Chem.* **276**, 33079-33085.

Okkema, P. G., Harrison, S. W., Plunger, V., Aryana, A. and Fire, A. (1993). Sequence requirements for myosin gene expression and regulation in *Caenorhabditis elegans*. *Genetics* **135**, 385-404.

Oldham, S., Bohni, R., Stocker, H., Brogiolo, W. and Hafen, E. (2000). Genetic control of size in *Drosophila*. *Philos. Trans. R. Soc. Lond. B. Biol. Sci.* **355**, 945-952.

Patterson, G. I., Koweek, A., Wong, A., Liu, Y. and Ruvkun, G. (1997). The DAF-3 Smad protein antagonizes TGF-β-related receptor signaling in the *Caenorhabditis elegans* dauer pathway. *Genes Dev.* **11**, 2679-2690.

Patterson, G. I. and Padgett, R. W. (2000). TGFβ-related pathways. Roles in *Caenorhabditis elegans* development. *Trends Genet.* **16**, 27-33.

Podos, S. D., Hanson, K. K., Wang, Y. C. and Ferguson, E. L. (2001). The DSmurf ubiquitin-protein ligase restricts BMP signaling spatially and temporally during *Drosophila* embryogenesis. *Dev. Cell* **1**, 567-578.

Qin, B., Lam, S. S. and Lin, K. (1999). Crystal structure of a transcriptionally active Smad4 fragment. *Structure Fold Des.* **7**, 1493-1503.

Qin, B. Y., Chacko, B. M., Lam, S. S., de Caestecker, M. P., Correia, J. J. and Lin, K. (2001). Structural basis of Smad1 activation by receptor kinase phosphorylation. *Mol. Cell* **8**, 1303-1312.

Raftery, L. A. and Sutherland, D. J. (1999). TGF-β family signal transduction in *Drosophila* development: from Mad to Smads. *Dev. Biol.* **210**, 251-268.

Ren, P., Lim, C. S., Johnsen, R., Albert, P. S., Pilgrim, D. and Riddle, D. L. (1996). Control of *C. elegans* larval development by neuronal expression of a TGF-β homolog. *Science* **274**, 1389-1391.

Savage, C., Das, P., Finelli, A. L., Townsend, S. R., Sun, C. Y., Baird, S. E. and Padgett, R. W. (1996). *Caenorhabditis elegans* genes sma-2, sma-3, and sma-4 define a conserved family of transforming growth factor β pathway components. *Proc. Natl. Acad. Sci. USA* **93**, 790-794.

Savage-Dunn, C. (2001). Targets of TGF β-related signaling in *Caenorhabditis elegans*. *Cytokine Growth Factor Rev.* **12**, 305-312.

Savage-Dunn, C., Tokarz, R., Wang, H., Cohen, S., Giannikas, C. and Padgett, R. W. (2000). SMA-3 smad has specific and critical functions in DBL-1/SMA-6 TGFβ-related signaling. *Dev. Biol.* **223**, 70-76.

Shi, Y., Hata, A., Lo, R. S., Massagué, J. and Pavletich, N. P. (1997). A structural basis for mutational inactivation of the tumour suppressor Smad4. *Nature* **388**, 87-93.

Shi, Y., Wang, Y. F., Jayaraman, L., Yang, H., Massagué, J. and Pavletich, N. P. (1998). Crystal structure of a Smad MH1 domain bound to DNA: insights on DNA binding in TGF-β signaling. *Cell* **94**, 585-594.

Souchelnytskyi, S., Tamaki, K., Engstrom, U., Wernstedt, C., ten Dijke, P. and Heldin, C. H. (1997). Phosphorylation of Ser465 and Ser467 in the C terminus of Smad2 mediates interaction with Smad4 and is required for transforming growth factor-β signaling. *J. Biol. Chem.* **272**, 28107-28115.

Sulston, J. E., Albertson, D. G. and Thomson, J. N. (1980). The *Caenorhabditis elegans* male: postembryonic development of nongonadal structures. *Dev. Biol.* **78**, 542-576.

Sulston, J. E. and Horvitz, H. R. (1977). Post-embryonic cell lineages of the nematode, *Caenorhabditis elegans*. *Dev. Biol.* **56**, 110-156.

Suzuki, Y., Yandell, M. D., Roy, P. J., Krishna, S., Savage-Dunn, C., Ross, R. M., Padgett, R. W. and Wood, W. B. (1999). A BMP homolog acts as a dose-dependent regulator of body size and male tail patterning in *Caenorhabditis elegans*. *Development* **126**, 241-250.

Wrana, J. L. and Attisano, L. (2000). The Smad pathway. *Cytokine Growth Factor Rev.* **11**, 5-13.

Wu, J. W., Hu, M., Chai, J., Seoane, J., Huse, M., Li, C., Rigotti, D. J., Kyin, S., Muir, T. W., Fairman, R., Massagué, J. and Shi, Y. (2001). Crystal structure of a phosphorylated Smad2. Recognition of phosphoserine by the MH2 domain and insights on Smad function in TGF-β signaling. *Mol. Cell* **8**, 1277-1289.

Xiao, Z., Liu, X., Henis, Y. I. and Lodish, H. F. (2000). A distinct nuclear localization signal in the N terminus of Smad 3 determines its ligand-induced nuclear translocation. *Proc. Natl. Acad. Sci. USA* **97**, 7853-7858.

Yochem, J., Gu, T. and Han, M. (1998). A new marker for mosaic analysis in *Caenorhabditis elegans* indicates a fusion between hyp6 and hyp7, two major components of the hypodermis. *Genetics* **149**, 1323-1334.

Yoshida, S., Morita, K., Mochii, M. and Ueno, N. (2001). Hypodermal expression of *Caenorhabditis elegans* TGF-β type I receptor SMA-6 is essential for the growth and maintenance of body length. *Dev. Biol.* **240**, 32-45.

Zhang, Y., Chang, C., Gehling, D. J., Hemmati-Brivanlou, A. and Derynck, R. (2001). Regulation of Smad degradation and activity by Smurf2, an E3 ubiquitin ligase. *Proc. Natl. Acad. Sci. USA* **98**, 974-979.

Zhu, H., Kavsak, P., Abdollah, S., Wrana, J. L. and Thomsen, G. H. (1999). A SMAD ubiquitin ligase targets the BMP pathway and affects embryonic pattern formation. *Nature* **400**, 687-693.